International Journal for Innovative Engineering and Management Research
PEER REVIEWED OPEN ACCESS INTERNATIONAL JOURNAL
www.ijiemr.org

COPY RIGHT

IJIEMR Transactions, online available on 30th Jul 2023. Link :http://www.ijiemr.org/downloads.php?vol=Volume-12&issue=Issue 06

10.48047/IJIEMR/V12/ISSUE 06/12

Title **An Improved Control strategy to suppress Double Frequency Oscillations in a Photovoltaic Grid-Tied Inverter with LVRT Capability**

Volume 12, ISSUE 06, Pages: 73-80

Paper Authors **P.Purnachander Rao, K.Prakash, M.Suryakalavathi**

International Journal for Innovative Engineering and Management Research
PEER REVIEWED OPEN ACCESS INTERNATIONAL JOURNAL
www.ijiemr.org

An Improved Control strategy to suppress Double Frequency Oscillations in a Photovoltaic Grid-Tied Inverter with LVRT Capability

P.Purnachander Rao[1], K.Prakash[2], M.Suryakalavathi[3]
[1]Research Scholar, Electrical and Electronics Engineering, JNTUH, Hyderabad
purnachander216@gmail.com
[2]Professor, Electrical and Electronics Engineering, Vaagdevi College of Engineering
prakashkams@gmail.com
[3]Professor, Electrical and Electronics Engineering, JNTUH, Hyderabad
munagala12@yahoo.co.in

Abstract— A novel control strategy for two-stage, three-phase Grid -Tied Photovoltaic (GTPV) systems is proposed in this paper to enhance the Power Quality under unbalanced grid faults. Power Quality related issues, such as injected currents and active and reactive power may be negatively impacted if a three-phase power converter operates under unbalanced grid voltage faults. The unbalanced fault causes double grid frequency oscillations in active power and reactive power and also injects non-sinusoidal currents into the grid. Similar variations in the DC-link voltage can occur in conventional two-stage GTPV inverters due to these double frequency oscillations of the injected active power. These oscillations of the dc-link voltage in such systems with an electrolytic capacitor can shorten the capacitor's lifespan and, consequently, the system as a whole. A method for creating a reference current, that can eliminate these oscillations at the dc-link and in the active power during unbalanced voltage sag, is a benefit of the proposed Low-Voltage Ride Through (LVRT) control strategy. Moreover, a reliable current limiting strategy is presented, that can proficiently anticipate overcurrent failure under grid faults. The performance of a 2-KW system using the proposed LVRT strategy is verified through MATLAB simulation.

Index Terms— Low-Voltage Ride-Through, Reference Current Generation, Dc-link voltage, Grid-Tied PV systems, Double frequency Oscillations, Voltage Sag;

I. INTRODUCTION

The adoption of Distributed Generation (DG) based Grid-Tied photovoltaic (GTPV) systems has grown exponentially in recent years [1] as a result of their benefits, including low cost of generation, absence of carbon emissions, improved grid reliability, and reduced network capacity. In order to reduce the negative effects of distributed generating resources, such as Photovoltaic (PV), Wind turbine systems, etc., on the power system, network operators regularly design and update grid codes [2]. LVRT capability is a crucial condition among various grid codes for Grid-Tied PV systems. Fundamentally, LVRT is a control capability that the Grid Tied PV inverters use to maintain utility connectivity during a drop in grid voltage [3-4].After the voltage has returned to its nominal value the active and reactive powers rebuilds to the pre-fault values. To support the grid's voltage, grid codes call for PVs to inject more reactive power. There are several ways to improve the fault ride through capabilities of PV systems by adding extra parts such as Energy Storage Systems, fault current limiters, and Static Synchronous Compensators (STATCOM) [5-7]. However, FACTS devices like STATCOM only inject reactive power to maintain the grid voltage during faults, while energy storage systems do not take the injection of reactive current into account [8-9].The addition of these hardware components also raises the system's total cost and complexity. Fuzzy logic control (FLC) and

optimization techniques, which aid in modifying the inverter's power references and enhancing the functionality of the inverter controller, have recently been applied by researchers [10-11]. Despite the fact that these computational techniques are effective and aid in solving the fault ride through issues, they increase the system's complexity. The improved inverter control techniques are garnering greater attention, in order to meet the grid code requirements with better precision and less expense [12]. Additionally, the system speed and dynamic responsiveness are improved with the employment of these updated inverter control techniques [13-14].

Photovoltaic Grid Tied Three-phase Inverter experiences the following issues under an unbalanced grid faults: 1) non sinusoidal injected currents, 2) oscillatory components are present in both the active power and the reactive power, and 3) Overcurrent tripping. As a result, various approaches to Current Reference Generation during grid faults have been discussed in the literature. The Instantaneous Active Reactive Control has been suggested in [15]. The Positive Sequence (PS) and Negative Sequence (NS) voltages are not utilized by the IARC, which only regulates three-phase voltages. This method produces currents with an acceptable Total Harmonic Distortion (THD) under normal conditions. However, unbalanced sags will result in high THD non-sinusoidal output currents. The Average Active-Reactive Control has been proposed in [16] to eliminate high order harmonics from the IARC method. For the purpose of determining the reference vectors for the active and reactive currents, this control strategy makes use of the average value of the three-phase voltages. However, the active power begins to oscillate at twice the grid fundamental frequency when active and reactive currents are injected in this approach.

In addition, the Positive and Negative Sequence Compensation (PNSC) has been proposed for injecting sinusoidal PS and NS currents in order to provide a particular active and reactive power [16]. Double grid frequency oscillations will reappear in the powers waveforms during unbalanced grid faults if the active and reactive power are injected simultaneously, which is the method's drawback. Injecting a set of balanced and sinusoidal currents containing PS components is done using the Balanced Positive Sequence Control method described in [16]. However, there are Double grid frequency components in both the active and reactive power. A control strategy has been presented in [17] that inject PS and NS components in proportion to a parameter that can be changed based on the grid fault. Under unbalanced faults, it is evident that the previous control methods experience either active power and dc-link voltage oscillation or the injection of non-sinusoidal currents into the grid. Due to the possibility of the dc-link capability failing, dc-link voltage oscillations in two-stage PV inverters can further reduce the inverter's lifespan [18-20].

II. PROBLEM ANALYSIS

The two-stage PV power converters' behavior under normal and abnormal grid conditions is examined in this section.

Figure.1 depicts a typical two-stage Grid-Tied three-phase system, which has an inverter and a boost converter connected by a capacitive dc-link. The Stationary Reference Frame (SRF) will be used to carry out the formulation. The conversion to the SRF from the three-phase system is as

$$v_{\alpha\beta} = \begin{bmatrix} v_\alpha \\ v_\beta \end{bmatrix} = \sqrt{\frac{2}{3}} \begin{bmatrix} 1 & -1/2 & -1/2 \\ 0 & \sqrt{3}/2 & \sqrt{3/2} \end{bmatrix} \begin{bmatrix} v_a \\ v_b \\ v_c \end{bmatrix} \quad (1)$$

Where v_a,v_b, and v_c are grid voltage vectors and v_α, v_β are the transformed voltages in the SRF on the α- and β-axes, respectively. It can be written similarly for current vectors.

The apparent power (S) can be determined using the parameters in the SRF as

International Journal for Innovative Engineering and Management Research
PEER REVIEWED OPEN ACCESS INTERNATIONAL JOURNAL
www.ijiemr.org

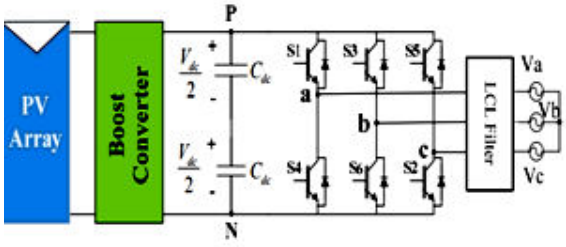

Fig.1. Two-stage three-phase grid-connected PV system.

$$S = v_{\alpha\beta}.{i_{\alpha\beta}}^{*} = \left(v_{\alpha\beta}^{+} + v_{\alpha\beta}^{-}\right).\left(i_{\alpha\beta}^{+} + i_{\alpha\beta}^{-}\right)^{*}$$
$$= v_{\alpha\beta}^{+}.{i_{\alpha\beta}^{+}}^{*} + v_{\alpha\beta}^{+}.{i_{\alpha\beta}^{-}}^{*}$$
$$+ v_{\alpha\beta}^{-}.{i_{\alpha\beta}^{+}}^{*} + v_{\alpha\beta}^{-}.{i_{\alpha\beta}^{-}}^{*} \quad (2)$$

where $v_{\alpha\beta}^{+}$ and $v_{\alpha\beta}^{-}$ are the PS and NS voltages in the SRF that can be derived from

$$v_{\alpha\beta}^{+} = \frac{1}{2}\begin{bmatrix} 1 & -q \\ q & 1 \end{bmatrix} v_{\alpha\beta} \quad (3)$$

$$v_{\alpha\beta}^{-} = \frac{1}{2}\begin{bmatrix} 1 & q \\ -q & 1 \end{bmatrix} v_{\alpha\beta} \quad (4)$$

where $q = e^{-j\pi/2}$ is a time-domain-applicable phase-shifting operator with a 90° lag. Additionally, $i_{\alpha\beta}^{+}$ and $i_{\alpha\beta}^{-}$ can be accomplished in a similar manner. The apparent power formulation contains four terms, the first of which can be written as

$$v_{\alpha\beta}^{+}.{i_{\alpha\beta}^{+}}^{*} = \left(v_{\alpha}^{+} + j\, v_{\beta}^{+}\right).\left(i_{\alpha}^{+} + j\, i_{\beta}^{+}\right)^{*}$$
$$= v_{\alpha}^{+}.i_{\alpha}^{+} + v_{\beta}^{+}.i_{\beta}^{+} + j(v_{\beta}^{+}.i_{\alpha}^{+} - v_{\alpha}^{+}.i_{\beta}^{+}) \quad (5)$$

The three other terms can all be obtained in a similar way. Clearly, a constant term in active and reactive power can be obtained by multiplying any two terms with identical sequences. On the other hand, multiplying any two terms with inverse sequences results in the oscillating parts of real and reactive power.

In summary, the powers can be estimated as

$$P = P_0 + \tilde{P} \quad (6)$$
$$P_0 = v_{\alpha}^{+}i_{\alpha}^{+} + v_{\beta}^{+}i_{\beta}^{+} + v_{\alpha}^{-}i_{\alpha}^{-} + v_{\beta}^{-}i_{\beta}^{-} \quad (7)$$
$$\tilde{P} = v_{\alpha}^{+}i_{\alpha}^{-} + v_{\beta}^{+}i_{\beta}^{-} + v_{\alpha}^{-}i_{\alpha}^{+} + v_{\beta}^{-}i_{\beta}^{+} \quad (8)$$
$$Q = Q_0 + \tilde{Q} \quad (9)$$
$$Q_0 = v_{\beta}^{+}i_{\alpha}^{+} - v_{\alpha}^{+}i_{\beta}^{+} + v_{\beta}^{-}i_{\alpha}^{-} - v_{\alpha}^{-}i_{\beta}^{-} \quad (10)$$
$$\tilde{Q} = v_{\beta}^{+}i_{\alpha}^{-} - v_{\alpha}^{+}i_{\beta}^{-} + v_{\beta}^{-}i_{\alpha}^{+} - v_{\alpha}^{-}i_{\beta}^{+} \quad (11)$$

In the above equations, P and Q are the total instantaneous real and reactive power, $P_0, Q_0, \tilde{P}$ and $\tilde{Q}$ are the constant and Oscillating parts in the real and reactive power, respectively.

Negative Sequence component is not present in the voltages or currents of the three phases during balanced voltage sag faults. Therefore, the real and reactive power waveforms lack oscillatory components, as shown by (6)-(11). According to the previous discussions, on the other hand, during unbalanced faults, the Negative Sequence component appears in three-phase voltages and currents, resulting in double grid frequency oscillations in the real or/and reactive power. The oscillations at the dc-link are caused by the oscillations at the real power, which have a negative effect on the dc-link capacitors' lifecycle.

III. PROPOSED CONTROL STRATEGY

The CRG method is discussed in detail in this section, followed by the current limitation method.

A. Generation of Reference Currents

Because the primary objective is to remove double grid frequency oscillations from the real power, equation (8) needs to be zero. The average amount of real and reactive power that must be delivered is equal to P_0 and Q_0. As a result, a typical formulation for producing sinusoidal currents is given as

$$i_{\alpha P} = \frac{v_{\alpha}^{+} - v_{\alpha}^{-}}{\left(v_{\alpha}^{+2} + v_{\beta}^{+2}\right) + k_{\alpha P}\left(v_{\alpha}^{-2} + v_{\beta}^{-2}\right)} P_0 \quad (12)$$

$$i_{\beta P} = \frac{v_{\beta}^{+} - v_{\beta}^{-}}{\left(v_{\alpha}^{+2} + v_{\beta}^{+2}\right) + k_{\beta P}\left(v_{\alpha}^{-2} + v_{\beta}^{-2}\right)} P_0 \quad (13)$$

$$i_{\alpha Q} = \frac{v_{\alpha\perp}^{+} + v_{\alpha\perp}^{-}}{\left({v_{\alpha\perp}^{+}}^{2} + {v_{\beta\perp}^{+}}^{2}\right) + k_{\alpha Q}\left({v_{\alpha\perp}^{-}}^{2} + {v_{\beta\perp}^{-}}^{2}\right)} Q_0 \quad (14)$$

$$i_{\beta Q} = -\frac{v_{\beta\perp}^{+} + v_{\beta\perp}^{-}}{\left({v_{\alpha\perp}^{+}}^{2} + {v_{\beta\perp}^{+}}^{2}\right) + k_{\beta Q}\left({v_{\alpha\perp}^{-}}^{2} + {v_{\beta\perp}^{-}}^{2}\right)} P_0 \quad (15)$$

$$\begin{bmatrix} v_{\alpha\perp} \\ v_{\beta\perp} \end{bmatrix} = \begin{bmatrix} 0 & -1 \\ 1 & 0 \end{bmatrix}\begin{bmatrix} v_{\alpha} \\ v_{\beta} \end{bmatrix} \quad (16)$$

In the above equations (12) to (16), $k_{\alpha P}, k_{\beta P}, k_{\alpha Q}, k_{\beta Q}$ are the parameters that can be either +1 or -1 to adjust the real

International Journal for Innovative Engineering and Management Research
PEER REVIEWED OPEN ACCESS INTERNATIONAL JOURNAL
www.ijiemr.org

and reactive current references in the Synchronous Reference Frame in accordance with grid requirement, $i_{\alpha P}$ and $i_{\beta P}$ are the reference active currents in the Synchronous Reference Frame, $i_{\alpha Q}$and $i_{\beta Q}$ are the reference reactive currents in the Synchronous Reference Frame, $v_{\alpha\perp}$ and $v_{\beta\perp}$ the orthogonal voltages of the Synchronous Reference Frame voltage vectors. In order to eliminate the double frequency oscillations in the active power and dc-link voltage, this paper will present a Current Reference Generation approach. As a result, the parameters are considered equivalent to -1.

B. Proposed Current Limiting Strategy

When voltage sag occurs in the grid, overcurrent is inevitable if the control is not changed, as was mentioned earlier. Therefore, in order to avoid overcurrent during LVRT operation, a fast and dependable control strategy ought to be used. A novel current limiting method that effectively limits currents to the nominal value is proposed in the following to achieve this objective.

When voltage sag is detected, the converter's rated power must be updated, which is called New Rated Capacity (NRC). Depending on the depth of the voltage sag, the NRC value typically falls below the converter's rated capacity during voltage sag faults. As a result, the NRC can be attained by

$$NRC = \frac{V^+ - V^-}{V_b} S \qquad (17)$$

Where S is the power converter's apparent or nominal power, V_b is the base voltage equal to the line-to-grid voltage's Root Mean Square (RMS) value, V^+ and V^- can be calculated as

$$V^+ = \sqrt{v_\alpha^{+2} + v_\beta^{+2}} \qquad (18)$$

$$V^- = \sqrt{v_\alpha^{-2} + v_\beta^{-2}} \qquad (19)$$

On the other hand, the reactive power required by the grid can be calculated as per the voltage sag dip.

$$\begin{cases} Q = 0 & if \quad V_{pu} > 0.9 \\ Q = S \times 1.5 \times (0.9 - V_{pu}) & if \quad 0.2 < V_{pu} < 0.9 \\ Q = 1.05 \times S & if \quad V_{pu} < 0.2 \end{cases} \qquad (20)$$

With V_{pu} being the residual voltage level and calculated as

$$V_{pu} = \frac{\sqrt{v_\alpha{}^2 + v_\beta{}^2}}{V_b} \qquad (21)$$

In equation (20), Q is the reactive power that must be delivered to the grid in response to voltage sag. To avoid overcurrent, the maximum permissible active power (Pmax) can be reached as follows:

$$P_{max} = \sqrt{\mathrm{NRC}^2 - \mathrm{Q}^2} \qquad (22)$$

From the above equations we can conclude that, once V_{pu} falls below 0.9 p.u., a fault in the grid is found by the control method. Then, the calculation works out the NRC and Q values by (17) and (20). P_{max}, which is how the maximum amount of real power that can be used is determined by under voltage sags; this is the maximum amount of real power that the converter can deliver to the grid. Throughout the fault period, P_{max} is continuously compared with the DC-link controller's active power reference (P^*). If $P_{max} > P^*$, the exact amount of active power that was previously injected into the grid can still be injected. On the other hand, if $P_{max} < P^*$, the inverter cannot inject the dc-link controller's output P^*. The non-MPPT mode is activated at this instance, and the PV power is reduced to P_{max}, to maintain a constant dc-link voltage.

C.Description of the Control Strategy

As depicted in Fig. 2. The capacitive dc-link's decoupling stage allows the two loops in the control structure to function independently. The dc-link voltage is adjusted with the help of a Proportional-Integral (PI) controller. Two Proportional-Resonant (PR) controllers are used in the current loop to control the SRF's currents. The voltage sag detection block generates a fault signal if V_{pu} falls below 0.9 per unit. The NRC, Q, and P_{max} calculator

International Journal for Innovative Engineering and Management Research
PEER REVIEWED OPEN ACCESS INTERNATIONAL JOURNAL
www.ijiemr.org

blocks are enabled at this instance by the fault signal. A comparator signal, which can be either 0 or 1, is then generated for the purpose of comparing P_{max} and P^*. The boost converter will operate in a non-MPPT mode when both the comparator signal and the fault signal are equal to 1 in an AND block. As a result, grid will be supplied with Q and the power converter will operate in the LVRT mode if the fault signal is greater than or equal to 1.

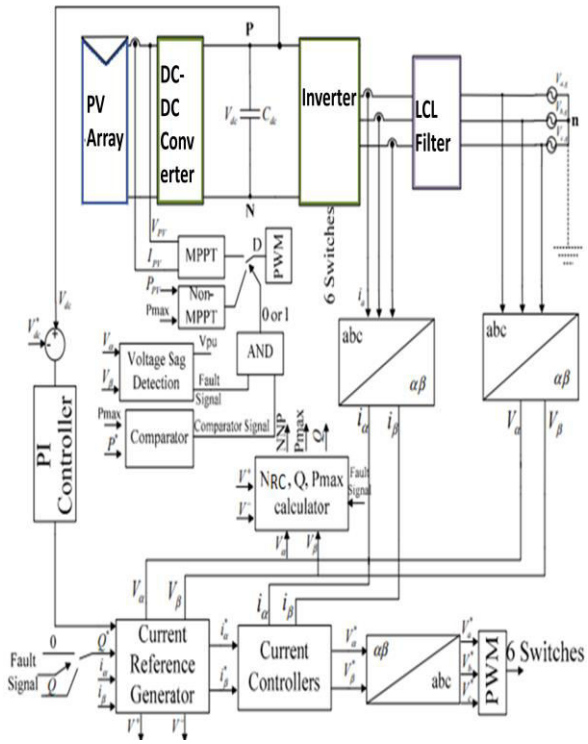

Fig.2. Block diagram of the proposed system

IV. SIMULATION RESULTS

A MATLAB/SIMULINK platform simulation setup is built to verify the performance of the proposed control scheme. Table. I shows the parameters of the power grid and the power converter.

TABLE.I
Parameters of the proposed system

Parameter	Value
Rated Power	2 KW
RMS value of the Grid Voltage	380 V
Filter Inductance (Inverter side)	6.85 mH
Filter Inductance(Grid side)	0.685 mH
Filter capacitance	2.4 μF
Switching frequency	16 KHz

In this work, an unbalanced fault is created at time t = 0.2 s, Phase voltages of the Grid V_b and V_c drop to 0.7 and 0.6 per unit, respectively, before rising to the nominal value at t = 0.3 s. The three-phase grid voltages are shown in Fig. 3 (a). The value of the fault signal will be equal to 1 after the controller recognises the voltage sag. The injected currents that are properly regulated by the suggested technique are shown in Fig. 3 (b) at the time of the fault. Phase-b and phase-c currents abruptly rise at the time of the fault and are thereafter limited to the rated value of 3.06 A. Even though the grid fault is imbalanced, Fig. 3 (b) confirms that the injected currents are entirely sinusoidal and limited to the rated magnitude.

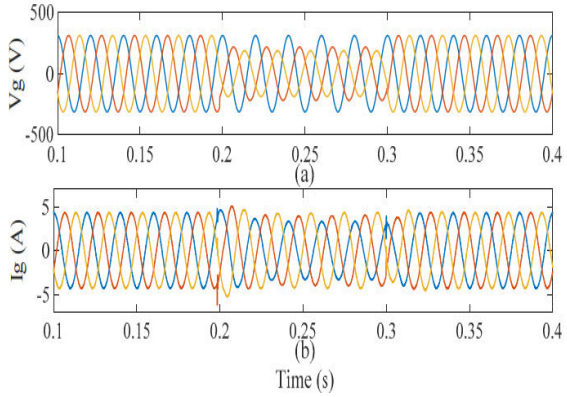

Fig. 3. Simulation results, (a) RMS voltages of the grid (b) currents injected into the grid.

Figure 4 illustrates, a simulated PNSC technique is used to confirm the advantages of the suggested approach. No current limitation approach is used for the PNSC scenario because the goal is to compare the output currents and power waveforms alone, not the values.

International Journal for Innovative Engineering and Management Research
PEER REVIEWED OPEN ACCESS INTERNATIONAL JOURNAL
www.ijiemr.org

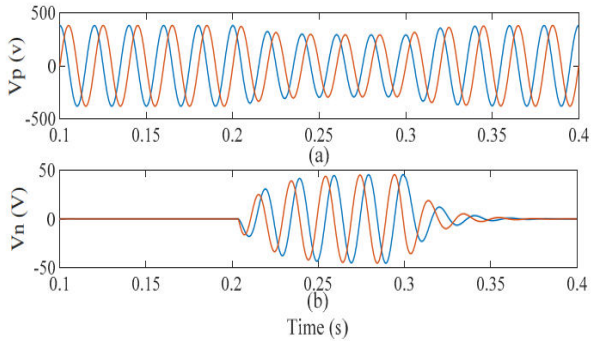

Fig.4. Simulation results of Positive and Negative phase sequence grid voltages

The injected currents, which are sinusoidal while the PNSC is in operation, are depicted in Fig. 5. However, Fig. 6(a) and Fig. 6(b) make it clear that double frequency oscillations are present in the dc-link voltage and active power waveforms.

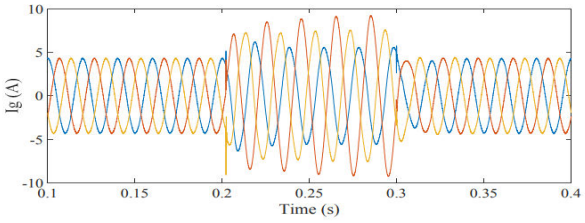

Fig.5. Three phase injected currents into the grid under an unbalanced fault with the PNSC control technique

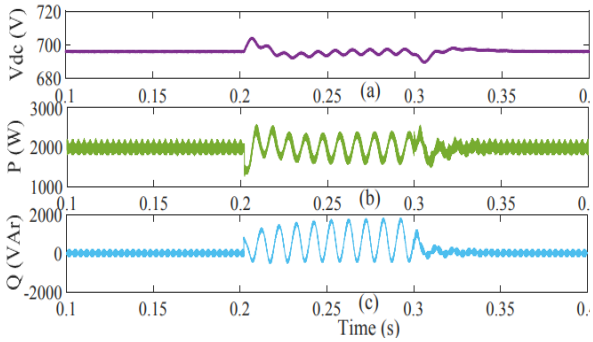

Fig.6. (a) voltage across the DC-link capacitor, (b) active power injected into the grid, and (c) Reactive power injected into the grid, under unbalanced fault with PNSC control technique.

The injected active power and reactive power with the suggested control approach are shown in Figs. 7(a) and 7(b), respectively. As seen in Fig.7, as soon as imbalanced voltage sag is identified, the active power is also decreased to avoid an overcurrent. The maximum permitted active power (P_{max}) is decreased when the fault occurs. Unlike the PNSC technique, the proposed control prevents Double frequency oscillations from occurring in the active power waveform even while the fault is imbalanced. On the other hand, after the fault signal is equal to 1, the reactive power injected into the grid rises.

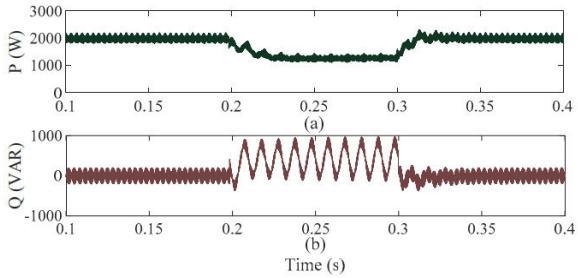

Fig.7. (a) active power injected into the grid, and (b) Reactive power injected into the grid, under unbalanced fault with proposed control technique.

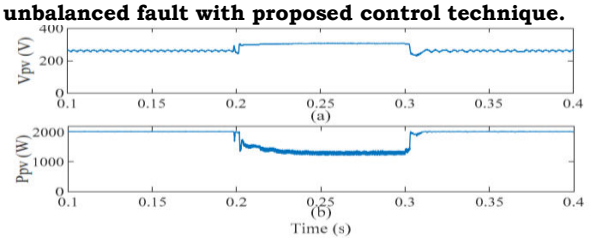

Fig. 8. Simulation results with proposed control technique under unbalanced voltage sag, (a) PV voltage and (b) PV power.

By switching from MPPT to non-MPPT mode, the power drawn from the PV arrays is decreased since the active power is decreased. The fault and comparator signals in Case Study B are equal to 1, which is the cause. As a result, the PV voltage rises and the PV power falls, as illustrated in Figs. 8(a) and 8(b).

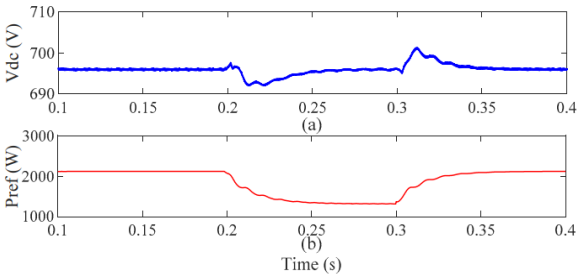

Fig. 9. Simulation results with proposed control technique under unbalanced voltage sag, (a) voltage across the DC-Link and (b) Power output of the DC-Link.

The dc-ink voltage drops at the time of the fault, as shown in Fig. 9(a). However, as shown in Fig. 9(b), the DC-Link controller eventually lowers the active power reference. The dc-link voltage is

correctly stabilized and recovered to a constant value, as shown in Fig. 9 (a).

V. CONCLUSION

To enhance the LVRT capability under unusual circumstances, this study has presented a novel control technique for the two-stage, three-phase three-wire PV Inverter. The proposed current limiting control method detects the voltage sag and responds to faults appropriately. In contrast to the PNSC technique, the most significant contribution of the suggested method is the elimination of the Double frequency oscillations in the dc-link voltage as well as the active power under unbalanced faults. Even with unbalanced faults, the injected currents generated by the controller are purely sinusoidal. The injected currents produced by the controller are solely sinusoidal, even with unbalanced faults. A more significant benefit is that the control structure has two operating modes, MPPT and Non-MPPT, both of which can function in abnormal circumstances. The paper's key addition is that the dc-dc converter now has a Non-MPPT operation mode. In contrast to modern current-limiting systems, this feature supports the simple current-limiting approach and correctly limits the currents to the rated value.

REFERENCES

1. Mar. 2014. [2] K. Mahmoud and M. Lehtonen, "Comprehensive analytical expressions for assessing and maximizing technical benefits of photovoltaics to distribution systems," IEEE Trans. Smart Grid, early access, Jul. 15, 2021, doi: 10.1109/TSG.2021.3097508.
2. I. I. Perpinias, N. P. Papanikolaou, and E. C. Tatakis, "Fault ride through concept in low voltage distributed photovoltaic generators for various dispersion and penetration scenarios," Sustain. Energy Technol. Assessments, vol. 12, pp. 15–25, Dec. 2015.
3. A. Q. Al-Shetwi and M. Z. Sujod, "Grid-connected photovoltaic power plants: A review of the recent integration requirements in modern grid codes," Int. J. Energy Res., vol. 42, no. 5, pp. 1849–1865, Apr. 2018.
4. V. L. Srinivas, B. Singh, and S. Mishra, "Fault ride-through strategy for two-stage grid-connected photovoltaic system enabling load compensation capabilities," IEEE Trans. Ind. Electron., vol. 66, no. 11, pp. 8913–8924, Nov. 2019.
5. M. Y. Worku and M. A. Abido, "Grid-connected PV array with supercapacitor energy storage system for fault ride through," in Proc. IEEE Int. Conf. Ind. Technol. (ICIT), Seville, Spain, Mar. 2015, pp. 2901–2906.
6. L. Chen, H. Chen, Y. Li, G. Li, J. Yang, X. Liu, Y. Xu, L. Ren, and Y. Tang, "SMES-battery energy storage system for the stabilization of a photovoltaic-based microgrid," IEEE Trans. Appl. Supercond., vol. 28, no. 4, Jun. 2018, Art. no. 5700407.
7. A. Q. Al-Shetwi, M. Z. Sujod, F. Blaabjerg, and Y. Yang, "Fault ridethrough control of grid-connected photovoltaic power plants: A review," Sol. Energy, vol. 180, pp. 340–350, Mar. 2019.
8. S. Xiangdong, R. Biying, Z. Qi, and A. Shaoliang, Solar Grid-Connected Photovoltaic Power Generation Technology (Low-Voltage Ride-Through Control Methods). New Delhi, India: Roy. Collins, 2020.
9. G. Lammert, Modelling, Control and Stability Analysis of Photovoltaic Systems in Power System Dynamic Studies. Kassel, Germany: Kassel Univ. Press, Jun. 2019.
10. N. H. Saad, A. A. El-Sattar, and A. E.-A. M. Mansour, "Improved particle swarm optimization for photovoltaic system connected to the grid with low voltage ride through capability," Renew. Energy, vol. 85, pp. 181–194, Jan. 2016.
11. F.-J. Lin, K.-C. Lu, T.-H. Ke, B.-H. Yang, and Y.-R. Chang, "Reactive power control of three-phase grid-connected PV system during grid faults using Takagi–Sugeno–Kang probabilistic fuzzy neural network control," IEEE Trans. Ind. Electron., vol. 62, no. 9, pp. 5516–5528, Sep. 2015.
12. Y. Zhang, J. Wang, H. Li, T. Q. Zheng, J.-S. Lai, J. Li, J. Wang, and Q. Chen, "Dynamic performance improving sliding-mode control-based feedback linearization for PV system under LVRT condition," IEEE Trans. Power Electron.,

vol. 35, no. 11, pp. 11745–11757, Nov. 2020.

13. I. R. S. Priyamvada and S. Das, "Online assessment of transient stability of grid connected PV generator with DC link voltage and reactive power control," IEEE Access, vol. 8, pp. 220606–220619, 2020.
14. Joshi, Jyoti, Anurag Kumar Swami, Vibhu Jately, and Brian Azzopardi. "A comprehensive review of control strategies to overcome challenges during LVRT in PV systems." *IEEE Access* 9 (2021): 121804-121834.
15. X. Zhao, J. M. Guerrero, M. Savaghebi, J. C. Vasquez, X. Wu, and K. Sun, "Low Voltage Ride-Through Operation of Power Converters in Grid-Interactive Microgrids by Using Negative-Sequence Droop Control," IEEE Transactions on Power Electronics, vol. PP, no. 99, pp. 1-1, 2016.
16. E. Afshari, G. R. Moradi, Y. Yang, B. Farhangi, and S. Farhangi, "A Review on Current Reference Calculation of Three-Phase Grid Connected PV Converters under Grid Faults," presented at the IEEE Power and Energy Conference at Illinois (PECI), Illinois, USA, 2017.
17. A. Junyent-Ferre, O. Gomis-Bellmunt, T. C. Green, and D. E. SotoSanchez, "Current control reference calculation issues for the operation of renewable source grid interface VSCs under unbalanced voltage sags," IEEE Transactions on Power Electronics, vol. 26, no. 12, pp. 3744-3753, 2011.
18. H. M. Hasanien, "An Adaptive Control Strategy for Low Voltage Ride Through Capability Enhancement of Grid-Connected Photovoltaic Power Plants," IEEE Transactions on Power Systems, vol. 31, no. 4, pp. 3230- 3237, 2016.
19. G. Ding, F. Gao, H. Tian, C. Ma, M. Chen, G. He, et al., "Adaptive DCLink Voltage Control of Two-Stage Photovoltaic Inverter During Low Voltage Ride-Through Operation," IEEE Transactions on Power Electronics, vol. 31, no. 6, pp. 4182-4194, 2016.
20. H. Wen and M. Fazeli, "A new control strategy for low-voltage ridethrough of three-phase grid-connected PV systems," J. Eng., vol. 2019, no. 18, pp. 4900–4905, Jul. 2019.